**Annales
Geophysicae**

Atmospheric wave induced O_2 and OH airglow intensity variations: effect of vertical wavelength and damping

H. Takahashi[1], A. Onohara[1], K. Shiokawa[2], F. Vargas[3], and D. Gobbi[1]

[1]Aeronomy division, Instituto Nacional de Pesquisas Espaciais, São José dos Campos, Brazil
[2]Solar Terrestrial Environment Laboratory, Nagoya University, Nagoya, Japan
[3]Department of Electrical and Computer Engineering, University of Illinois at Urbana-Champaign, Urbana, USA

Abstract. From nocturnal variations of the airglow O_2 (0-1) and OH Meinel (6-2) band emission intensity and the rotational temperature, gravity waves and the damping effect in the MLT region were investigated. The data set was obtained from photometer measurements at Rikubetsu (43.5° N, 143.8° E), Japan, from March 2004 to August 2005. The ratio of the amplitude of oscillation and their phase difference between the two emissions were calculated when simultaneous periodic variations were observed. The ratio showed a linear correlation with the phase difference. The vertical wavelength and damping rate were estimated by using a model calculation carried out by previous works. The results show that the wave damping is significant when the vertical wavelength is shorter than 30–40 km. Krassovsky's parameter η, which represents a ratio between the emission intensity and temperature oscillations, was also calculated. The results show that the η also depends on the damping effect.

Keywords. Atmospheric composition and structure (Airglow and aurora)

1 Introduction

Atmospheric tidal and gravity wave propagations in the upper mesosphere and lower thermosphere (MLT) region are highly variable. In this region, many of the waves start to break because of exponential growth of the wave amplitude and also due to background wind systems. The gravity wave saturation spectrum has been studied by, i.e., Fritts (1984), Dewan and Good (1986) and Smith et al. (1987) and observed by MST radar (i.e., Tsuda et al., 1989). The momentum of saturated waves is transferred into the background

wind, depositing the wave energy into the atmosphere (Garcia and Solomon, 1985; Fritts and Alexander, 2003). The measurement of gravity waves in the MLT region requires observation of the sky in a two-dimensional form and relatively high temporal resolution (in a few minutes). Among several techniques, radio frequency and optical measurements, airglow observations using a photometer and all-sky imagers have been effectively used. (Hecht et al., 1987; Taylor et al., 1991, 2009; Takahashi et al., 1992; Taori and Taylor, 2006).

Airglow OH and O_2 emissions provide useful information on the variation of the hydrogen-oxygen chemistry and the temperature field. Since the OH emission layer is normally located at around 87 km (Baker and Stair, 1988) and O_2 (0-1) band emission layer at 94 km (Murtagh et al., 1990), simultaneous measurement of the two emissions leads us to investigate the vertical wave propagation feature of gravity and tidal waves. For this purpose, Krassovsky's parameter "η", a ratio of the amplitude of temporal variation of the emission rate and the associated rotational temperature, has been used (Krassovsky, 1972; Taori and Taylor, 2006). The parameter "η" has been termed as a complex quantity, defined as $\eta = |\eta|e^{-i\Phi}$, where $|\eta|$ indicates the ratio of the amplitudes of variation between the emission intensity and temperature and Φ is a phase difference between them. It depends on the wave period and horizontal wavelength (e.g., Schubert et al., 1991). Therefore, it has been used to retrieve wave parameters. Many works on the gravity wave and tides using the η values have been written (Walterscheid et al., 1987; Hickey, 1988a, b; Reisin and Scheer, 1996; Taori and Taylor, 2006). However, η includes various other unknown parameters, such as the variation of local oxygen photochemistry (Hickey et al., 1993), and height variation of the emission layer which affects emission rates and temperature directly (Liu and Swenson, 2003; Vargas et al., 2007).

The gravity wave dissipating process in the MLT region will be another important factor to be considered in studying

the variability of η. Schubert et al. (1991) demonstrated the importance of eddy diffusion in η in their model calculation. Taori et al. (2007) pointed out the effects of wave growth and dissipation in the O_2 and OH emissions. Liu and Swenson (2003) pointed out that η depends on the vertical wavelength and also the wave damping effect. From their model calculation, they further suggested that the vertical wavelength and damping rate of gravity waves can be derived from the simultaneous measurements of the O_2 and OH emission rates. Vargas et al. (2007) extended the model calculation of gravity wave effects on the airglow emission rates, including the OI 557.7 nm emission in addition to the O_2 and OH emissions.

In the present study, we investigate temporal variations of the O_2 and OH emission rates, the phase difference and variability of amplitude of oscillation. From the relation between the amplitude of oscillation and vertical wavelength obtained by Vargas et al. (2007), we also estimated the vertical wavelength of the observed short period (2–10 h) oscillations and the wave damping effect. The discussion will be focused on the wave damping rate in the MLT region. Krassovsky parameters have also been calculated and studied in their dependence on the damping effect.

2   Observations

The atmospheric O_2b (0-1) band, hereafter O_2, and hydroxyl OH Meinel (6-2) band, hereafter OH, airglow spectral measurements have been conducted at Rikubetsu (43.5° N, 143.8° E), Japan, since March 2004 using a new airglow spectral imaging photometer (No. 3 in series) with a cooled-CCD detector, developed by Solar-Terrestrial Environment Laboratory (STEL), Nagoya University. The photometer characteristics, data processing, and the rotational temperature calibration procedure have been reported by Shiokawa et al. (2007). The rotational line spectrum of the O_2 and OH bands formed by a narrow band interference filter and lens system is focused on a cooled CCD camera. The line intensities can be obtained by integrating the ring pattern spectrum. The rotational temperatures extracted from the line spectrum of OH and O_2 spectra were compared with Na lidar temperature at Platteville, Colorado (40.2° N, 255.3° E), in September 2003. A good linear correlation between the two temperatures was found, but with a bias. Hence, the rotational temperatures were corrected using the Na lidar temperature by Shiokawa et al. (2007).

For the present study, the data obtained from March 2004 to August 2005 (18 months), a total of 146 clear-sky nights of data for O_2 and 155 nights for OH, were used. The sky condition was checked using sky images obtained by a collocated all-sky imager. Nocturnal variation time series longer than 4 h were selected for the present analysis. The time series with a lack of data within 5 min were interpolated for spectral analysis.

Nocturnal variations of the intensity and temperature were submitted to Lomb Scargle spectral analysis in order to find periodic oscillations in the time series. The spectral analysis frequently revealed two or more frequencies in the time series. In order to calculate amplitude and phase of the first oscillation mode, which normally has a period of longer than 6 h, a least mean square fitting with a second order polynomial was adapted. Once calculated, the amplitude and phase of the second order polynomial was subtracted from the original data, so that a higher order frequency oscillation appeared. For this residual oscillation, a sinusoidal function was applied to find out the amplitude and phase for the second order oscillation. This way, we found 47 nights of observation with periodic oscillation in the O_2 emission and 75 nights for OH emission. However, among them we found only 19 nights of observation when the two emissions showed the same period of oscillation within an error range of less than 20%.

The Krassovsky parameter η and the phase shift Φ of the O_2 and OH oscillations were calculated when both the intensity and temperature oscillations had the same oscillation period (within an error range of $\pm 15\%$). Moreover, the correlation coefficient between the adjusted curve and the data series should be better than 0.5. The steps used for the calculation of η and Φ are similar to those reported in the early works (Taori and Taylor, 2006).

3   Results

The wave characteristics (period and phase) and Krassovsky parameter η for O_2 and OH were calculated for an individual night. In practice, it was difficult to retrieve more than two harmonic oscillations. Only the oscillation found in both the intensity and temperature variations was used in the present study. In Figs. 1, 2 and 3 nocturnal variations and the polynomial curve fitting of the O_2 and OH emission intensity and the rotational temperature were plotted as examples. The long period components (longer than 24 h) have been subtracted. Figure 1 depicts an example of a short period oscillation (2.8 ± 0.2 h). Only the amplitudes of oscillation, I'/I_0 and T'/T_0, where I' and T' indicate the amplitude of oscillation and I_0 and T_0 indicate averaged values during the period, are plotted. Sinusoidal oscillations can be seen in both the O_2 and OH emission intensity and temperature variations. Both O_2 and OH show phase differences between the intensity and temperature, the temperature leading intensity by 0.5–0.7 h. In addition to it, O_2 leads OH by ~0.8 h, suggesting that a gravity wave is propagating upward (phase propagating downward) passing in the emission layers. Krassovsky's η value was obtained from a ratio of the amplitudes of oscillation of the emission intensity and temperature, $(I'/I_0)/(T'/T_0)$, and the phase difference between them (Φ). In this case, $|\eta|$ for O_2 and OH is 5.1 and 14.0, respectively. It is interesting to note that the amplitude

Table 1. $O_2b(0-1)$ and OH(6-2) intensity oscillation period, relative amplitude and phase difference between OH and O_2 for 20 wave events observed at Rikubetsu, Japan, in 2004–2005.

Day 2004–2005	Period (h)	O_2 int. Ampl.	OH int. Ampl.	Phase diff. (deg.)
18 Mar	2.3	0.124	0.065	131
20 May	3.1	0.117	0.052	35
18 Aug	3.5	0.279	0.360	83
22 Aug	2.8	0.098	0.121	103
23 Aug	4.7	0.156	0.196	107
25 Aug	5.8	0.286	0.216	37
16 Sep	4.1	0.075	0.086	124
17 Sep	10.6	0.350	0.200	20.6
8 Oct	2.8	0.041	0.076	190
17 Oct	10.6	0.251	0.297	95
13 Nov	6.1	0.142	0.135	90
15 Nov	7.8	0.370	0.128	0
18 Nov	8.4	0.777	0.591	59
7 Dec	6.9	0.473	0.174	21
9 Dec	9.9	0.324	0.409	39.6
14 Dec	10.9	0.423	0.236	93
9 Jan	8.4	0.268	0.130	42
9 Jan	4.5	0.061	0.061	40
2 Feb	6.7	0.130	0.142	91
13 Mar	3.0	0.020	0.072	156

of oscillation of O_2 is 0.098, which is less than that of OH (0.121). If this oscillation was generated by a gravity wave and no dissipation of wave energy happened, the amplitude of oscillation of O_2 might be expected to be larger than that of OH, because of that the emission height of O_2 is higher than OH by about 6–7 km, almost one scale height and the gravity wave amplitude should increase with height. Less amplitude of the oscillation of O_2 indicates that the wave amplitude was reduced from 87 km to 94 km of altitude.

An example of a long period (∼10 h) oscillation can be seen in Fig. 2. The long period oscillation (10.8 h) suggests that this could be a signature of semidiurnal tide. The phase lag of OH against O_2 is large, around 2.5 h. The amplitude of oscillation of O_2 (0.423) is larger than that of OH (0.236), what suggests that the wave amplitude increased with height. Figure 3 presents a case in which the phase difference between the O_2 and OH is null. In the case of the OH emission intensity and temperature, there is no phase lag between them. In the case of the O_2 emission intensity and its temperature, however, a phase lag of about 1.0 h can be seen. No phase difference between the two emissions indicates that the wave must be in an evanescent form. The amplitude of oscillation of O_2 (0.370) is larger than OH (0.128) with a factor of 2.9. This is close to what we expect in the case of no dissipation of the wave amplitude from the OH to O_2 emission heights, as mentioned in the next section.
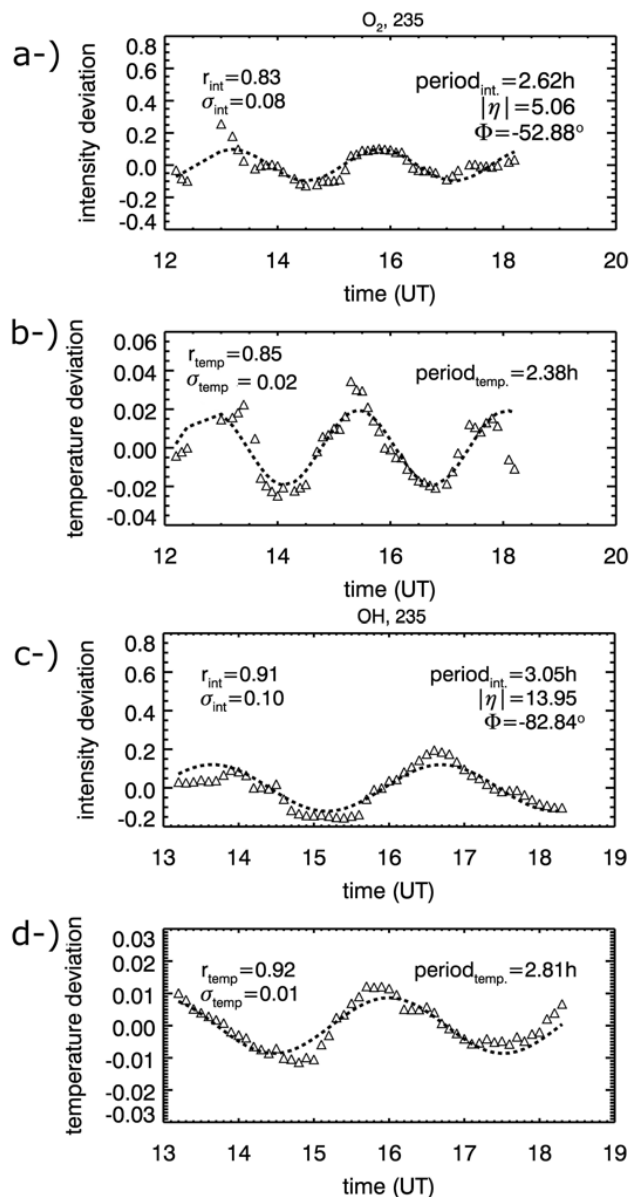

Fig. 1. Normalized nocturnal variations of O_2b emission intensity **(a)** and the rotational temperature **(b)**, the OH(6-2) emission intensity **(c)** and the temperature **(d)** in the night of 22 August 2004. The dashed lines are least mean square fitting using harmonic analysis. "r" and "σ" indicate respectively correlation coefficient and STD deviation between the observed and fitting. "η" and "Φ" represent, respectively, Krassovsky coefficient and the phase difference between the intensity and temperature variations. The local midnight is 15:00 UT.

The observed period, phase and amplitudes of the emission intensity and temperature for the 19 nights when both emissions showed the same oscillation mode are summarized in Table 1. Although the number of night of observation with periodic oscillations in O_2 and OH is large, the number of case with both emissions demonstrate the same
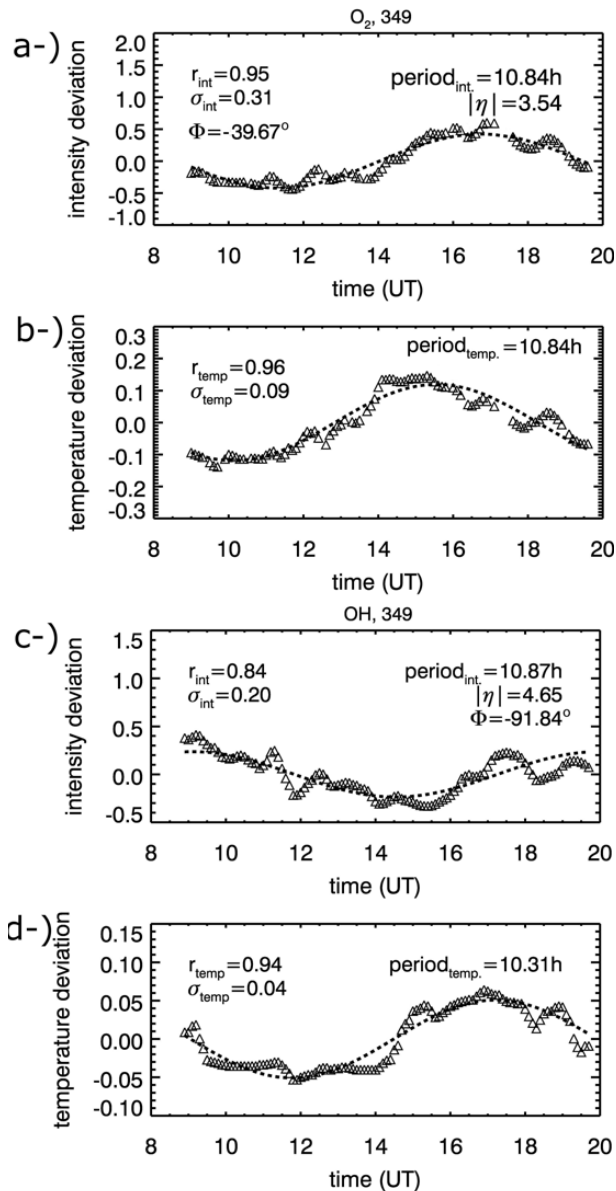
Fig. 2. As same as Fig. 1, but for 14 December 2004.

Fig. 3. As same as Fig. 1, but for 15 November 2004.

periodic oscillation is limited by only 20 cases in the present work. The relation between η and period has been studied by Onohara et al. (2010). In the present work, we focus our discussion in the amplitude of oscillation of the O_2 and OH emission rates which reflects the gravity wave growth and/or dissipation effect in the MLT region. In order to investigate it, we plot, in Fig. 4, ratios of the oscillation amplitude of the O_2 and OH emission intensities as a function of the phase difference between the two emissions. The ratio varied from 0.27 to 2.9. The negative trend indicates that when the phase difference is small, normally for a longer period of oscillation, the ratio is high, i.e., larger amplitude of variation in O_2 than that of OH.
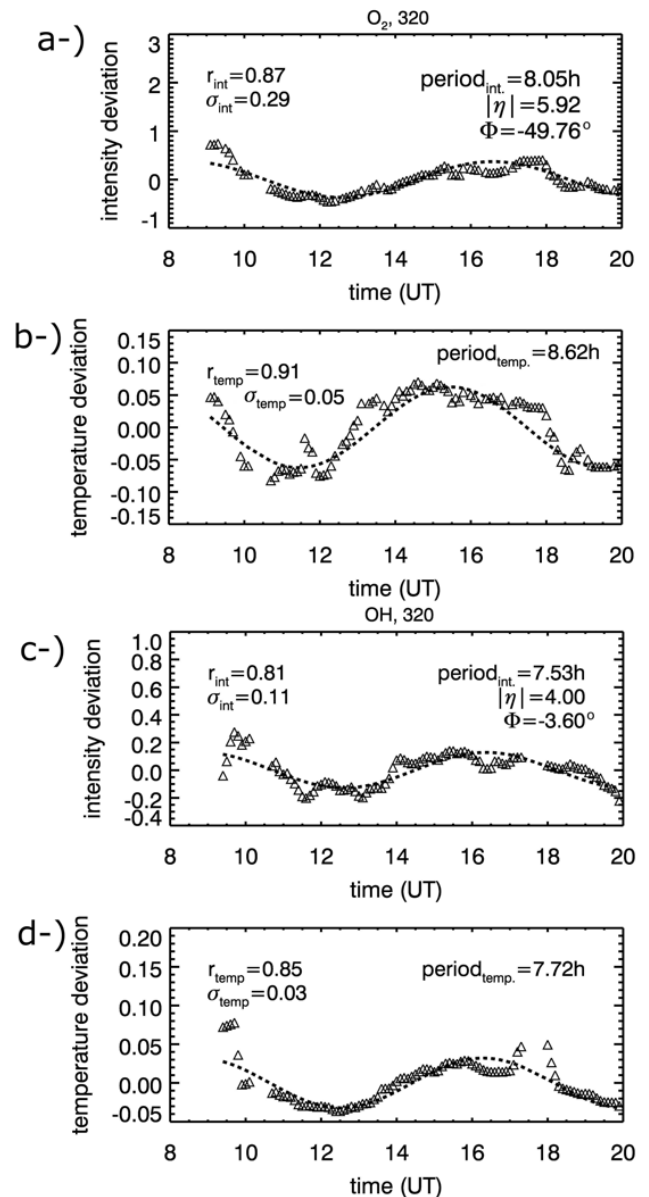
According to the model calculations of Liu and Swenson (2003) and Vargas et al. (2007), the phase difference between the two emissions is a function of vertical wavelength. It is not sensitive to the period of variation (Vargas et al., 2007). Using relationship between the phase difference and the vertical wavelength presented by Vargas et al. (2007), Fig. 4 can be re-plotted as a function of vertical wavelength, which is presented in Fig. 5. It can be noticed that the estimated wavelengths are in a range of 15 to 100 km. The linear relation indicates that the ratio is small for the short vertical wavelength and large for the longer wavelength. A higher ratio means that the O_2 oscillation amplitude is larger than that of OH, increasing with the longer vertical wavelength. For the
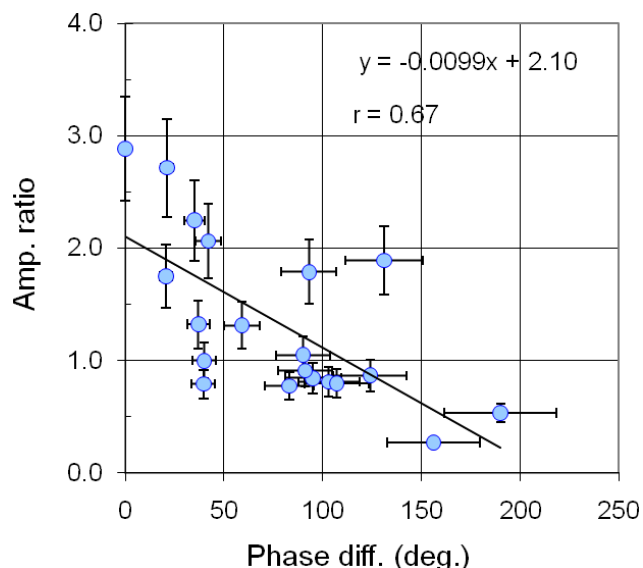
Fig. 4. Ratio of amplitude of oscillation between the O_2 and OH emission intensities against the phase difference between the two emissions. The straight line is a linear regression curve and "r" represents the correlation coefficient.
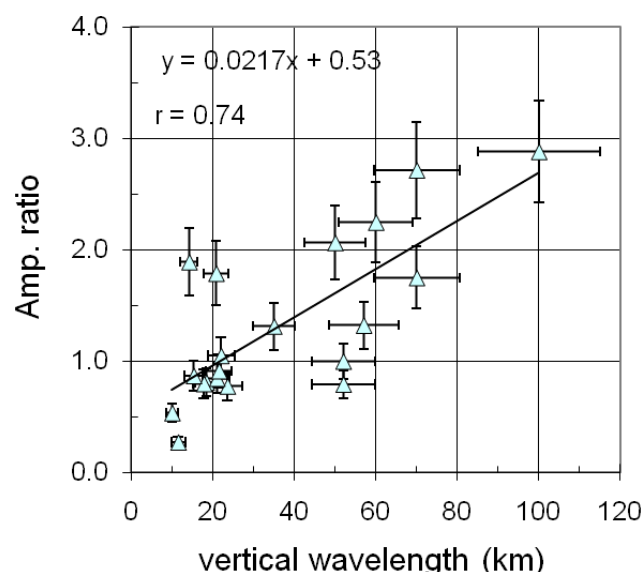

Fig. 5. Relation between the ratios of the O_2 and OH emission intensity variations and the vertical wavelengths. The straight line is a linear regression curve and "r" indicates the correlation coefficient.

shorter vertical wavelength, less than 20 km, the ratio is less than 1 which indicates that the wave amplitude was significantly reduced in the O_2 emission height. The fact of the ratio being dependent on the vertical wavelength is worthwhile to be further investigated.

4 Discussion

4.1 Wave damping effect in the O_2 and OH emission intensity variations

The variability of the ratio between the O_2 and OH emission intensity variation amplitude suggests a damping effect in the height region from the OH layer ($\sim$87 km) to O_2 layer ($\sim$94 km). Gravity wave breaking effects in the MLT region (80–100 km) have been extensively studied (Fritts et al., 2006). From the O_2 and OH airglow observation, gravity wave growth and dissipation were first studied by Noxon (1978), and later by Reisin and Scheer (1996). Recently Taori et al. (2007) demonstrated the variability of wave growth rate from the OH and O_2 emission intensity temporal variations. Liu and Swenson (2003) and Vargas et al. (2007) first tried to estimate the damping rate by using O_2 and OH emission intensity variations in their atmospheric models. The wave damping rate β can be defined in a term of wave amplitude:

$$A(z) = A_0 \exp((1-\beta)z/2H),$$

where A is amplitude of oscillation, z is altitude (the height difference of the OH and O_2 emission layers) and H is a

scale height. If β is 0, the wave has no dissipation and freely propagating vertically. If the height difference z is 7 km and the scale height is around 6.0 km in this region, the wave amplitude growth rate is around 3.0. When β is one, the wave is saturated and the amplitude does not increase with height. If β is larger than one, then the wave amplitude decreases with altitude. According to their model estimation, wave damping is related to the ratio and vertical wavelength. Based on the relation calculated by Vargas et al. (2007), the damping rates of the present work have been obtained and plotted in Fig. 6. The damping rates varied from around 0 (no damping) to 4 (strongly damped). A major part of cases, when the vertical wavelength was between 20 and 50 km, the damping rates were within 1 (no growth of amplitude) and 2.5. It indicates that most of the waves, in our present case, were saturated or damped. It suggests that the gravity waves of the vertical wavelength shorter than 50 km mostly dissipate and deposit the momentum in the background wind field in the height region above the OH emission layer.

4.2 Krassovsky parameter and damping rate

The Karssovsky value η depends on the wave period and horizontal wavelength. η for OH has been calculated by Schubert et al. (1991) and for O_2 by Hickey et al. (1993). Since then, many works have focused their investigations on the variability of η and the phase difference (Φ) between the intensity and temperature variations against the gravity wave parameters. Onohara et al. (2010) plotted η and Φ as a function of period. They found, however, no strong dependency of η on the oscillation period, rather they found it showing
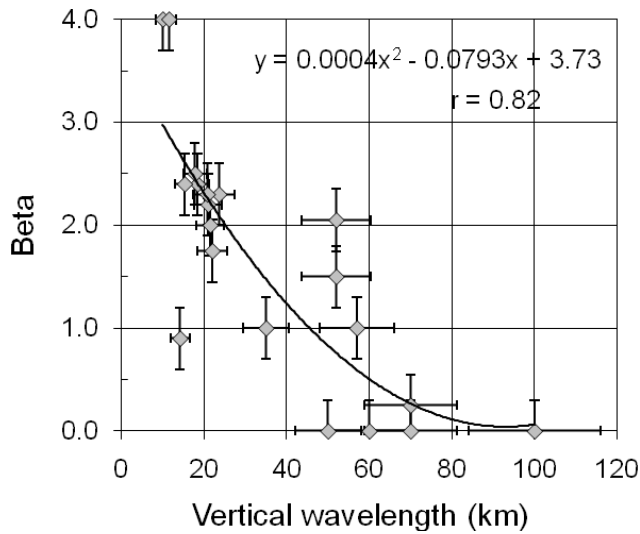
Fig. 6. Wave damping rate as a function of the vertical wavelength for each wave event observed, based on the Fig. 6a by Vargas et al. (2007). The fitted line is polynomial fitting and "r" indicates the correlation coefficient.
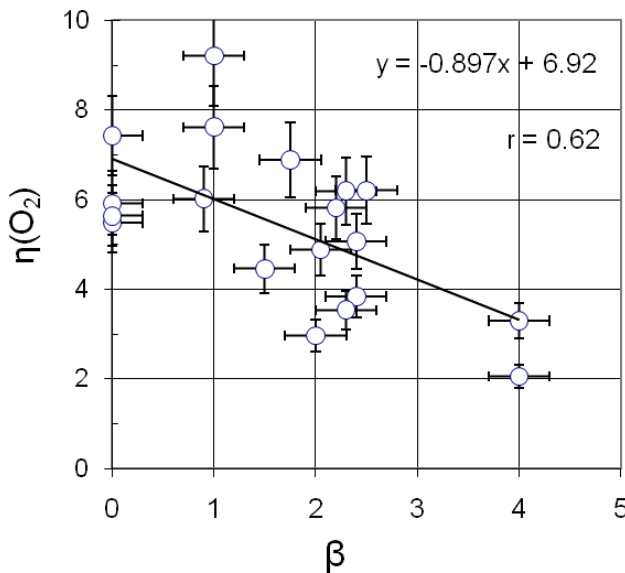

Fig. 7. Relation between the Krassovsky parameters (η) and damping rates (β) of the O_2 emission. The straight line is a linear regression curve and "r" indicates the correlation coefficient.

a much scattered form. Some other factors should be taken in account to explain it. In the present study, therefore, we plotted η as a function of β, which is shown in Fig. 7 for the case of the O_2 emission. η shows a tendency of decrease with an increasing damping rate. The η is around 6 to 7 when the damping rate is 0 (no dissipation), and decreases to 2 to 3 with larger damping. This means that η is partly a function of β. This might be a reason why the η values are scattered against the wave period in the previous works.

5 Conclusions

From the amplitude of periodic oscillations of the O_2b (0-1) and OH (6-2) emission rates, we calculated the amplitude ratio and phase difference between them. When the phase difference increased (for shorter vertical wavelength), we noticed that the ratio decreased, i.e., the amplitude of oscillation of O_2 decreased more than that of OH. The damping rate, estimated using the Vargas et al. (2007) model, varied from 0 (no dissipation) to >3 (strongly dissipated), depending on the vertical wavelength. The present results demonstrate that the gravity waves with the vertical wavelength shorter than 20–30 km significantly reduce the wave amplitude, due to the dissipation process in the MLT region. The Krassovsky parameter (η) partly depends on the wave damping rate (β).

References

Baker, D. J. and Stair, J. A. T.: Rocket Measurements of the Altitude Distributions of the Hydroxyl Airglow, Physica Scripta, 37, 611–622, 1988.

Dewan, E. M. and Good, R. E.: Saturation and the "universal" spectrum for vertical profiles of horizontal scalar winds in atmosphere, J. Geophys. Res., 91, 2742–2748, 1986.

Fritts, D. C.: Gravity wave saturation in the middle atmosphere – A review of theory and observations, Rev. Geophys. Space Phys., 22, 275–308, 1984.

Fritts, D. C. and Alexander, M. J.: Gravity wave dynamics and effects in the middle atmosphere, Rev. Geophys., 41(1), 1–46, 2003.

Fritts, D. C., Vadas, S. L., Wan, K., and Werne, J. A.: Mean and variable forcing of the middle atmosphere by gravity waves, J. Atmos. Sol. Terr. Phys., 68, 247–265, 2006.

Garcia, R. and Solomon, S.: The effect of breaking gravity waves on the dynamics and chemical composition of the mesosphere and lower thermosphere, J. Geophys. Res., 90(D2), 3850–3868, 1985.

Hecht, J. H., Walterscheid, R. L., Sivjee, G. G., Christensen, A. B., and Pranke, J. B.: Observations of wave-driven fluctuations of OH nightglow emission from Sondre Stromfjord, Greenland, J. Geophys. Res., 92(A6), 6091–6099, 1987.

Hickey, M. P.: Effects of eddy viscosity and thermal conduction and coriolis force in the dynamics of gravity wave driven fluctua-

tions in the OH nightglow, J. Geophys. Res., 93(A5), 4077–4088, 1988a.

Hickey, M. P.: Wavelength dependence of eddy dissipation and coriolis force in the dynamics of gravity wave driven fluctuations in the OH nightglow, J. Geophys. Res., 93(A5), 4089–4101, 1988b.

Hickey, M. P., Schubert, G., and Walterscheid, R. L.: Gravity wave-driven fluctuations in the O_2 atmospheric (0-1) nightglow from an extended, dissipative emission region, J. Geophys. Res., 98(A8), 13717–13729, 1993.

Krassovsky, V. I.: Infrasonic variations of OH emission in the upper atmosphere, Ann. Geophys., 28, 739–746, 1972.

Liu, A. Z. and Swenson, G. R.: A modeling study of O2 and OH airglow perturbations induced by atmospheric gravity waves, J. Geophys, Res., 108(D4), 4151, doi:10.1029/2002JD002474, 2003.

Murtagh, D. P., Witt, G., Stegman J., McDade, I. C., Llewellyn, E. J., Harris, F., and Greer, R. G. H.: An Assessment of Proposed O(1S) and O2(b) Nightglow Excitation Parameters, Planet. Space Sci., 38, 43–53, 1990.

Noxon, J. F.: Effect of Internal Gravity Waves Upon Night Airglow Temperatures, Geophys. Res. Lett., 5, 25–27, 1978.

Onohara, A., Takahashi, H., Gobbi, D., and Shiokawa, K.: Krassovsky η parameter calculated by using O_2(0-1) and OH(6-2) airglow emissions, Rev. Bras. Geofísica, 28(4), 579–592, 2010.

Reisin, E. R. and Scheer, J.: Characteristics of atmospheric waves in the tidal period range derived from zenith observations of O_2(0,1) atmospheric and OH (6,2) airglow at lower mid-latitudes, J. Geophys. Res., 101(D16), 21223–21232, 1996.

Schubert, G., Walterscheid, R. L., and Hickey, M. P.: Gravity wave-driven fluctuations in OH nightglow from an extended, dissipative emission region, J. Geophys. Res., 96(A8), 13869–13880, 1991.

Shiokawa, K., Otsuka, Y., Suzuki, S., Katoh, T., Katoh, Y., Satoh, M., Ogawa, T., Takahashi, H., Gobbi, D., Nakamura, T., Williams, B. P., She, C. Y., Taguchi, M., and Shimomai, T.: Development of airglow temperature photometers with cooled-CCD detectors, Earth, Planet Sci., 59, 585–599, 2007.

Smith, S. A., Fritts, D. C., and VanZandt, T. E.: Evidence for a saturated spectrum of Atmospheric gravity waves, J. Atmos. Sci., 44(10), 1404–1410, 1987.

Takahashi, H., Sahai, Y., Batista, P. P., and Clemesha, B. R.: Atmospheric gravity wave effect on the airglow O2(0,1) and OH(9,4) band intensity and temperature variations observed from a low latitude station, Adv. Space Res., 12(10), 131–134, 1992.

Taori, A. and Taylor, M.: Characteristics of wave induced oscillations in mesospheric O_2 emission intensity and temperatures, Geophys. Res. Lett., 33, L01813, doi:10.1029/2005GL024442, 2006.

Taori, A., Guharay, A., and Taylor, M. J.: On the use of simultaneous measurements of OH and O_2 emissions to investigate wave growth and dissipation, Ann. Geophys., 25, 639–643, doi:10.5194/angeo-25-639-2007, 2007.

Taylor, M. J., Espy, P. J., Baker, D. J., Sica, R. J., Neal, P. C., and Pendleton, W. R.: Simultaneous intensity, temperature and imaging measurements of short period wave structure in the OH nightglow emission, Planet. Space Sci., 39, 1171–1188, 1991.

Taylor, M. J., Pautet, P.-D., Medeiros, A. F., Buriti, R., Fechine, J., Fritts, D. C., Vadas, S. L., Takahashi, H., and São Sabbas, F. T.: Characteristics of mesospheric gravity waves near the magnetic equator, Brazil, during the SpreadFEx campaign, Ann. Geophys., 27, 461–472, doi:10.5194/angeo-27-461-2009, 2009.

Tsuda, T., Inoue, T., Fritts, D. C., VanZandt, T. E., Kato, S., Sato, T., and Fukao, S.: MST radar observations of a saturated gravity wave spectrum, J. Atmos. Sci., 46(15), 2440–2447, 1989.

Vargas, F., Swenson, G., Liu, A., and Gobbi, D., O(1S), OH, and O2(b) airglow layer perturbations due to AGWs and their implied effects on the atmosphere, J. Geophys, Res., 112, D14102, doi:10.1029/2006JD007642, 2007.

Walterscheid, R. L., Schubert, G., and Straus, J. M.: A dynamical-chemical model of wave driven fluctuations in the OH nightglow, J. Geophys. Res., 92(A2), 1241–1254, 1987.